Feed-Forward Control of an HVDC Power Transmission Network

Christian Schmuck, Frank Woittennek, Albrecht Gensior, and Joachim Rudolph, *Member, IEEE*

***Abstract*— An efficient and well-established technology for power transmission across long distances is high-voltage direct current transmission (HVDC). However, HVDC is currently almost completely limited to peer-to-peer connections or networks with peers situated closely to each other. This contribution introduces the flatness-based design of a feed-forward control of HVDC transmission networks comprising two or more converter stations. The resulting control concept allows for a flexible determination of the power distribution within the network. Furthermore, effects such as power losses and delays due to wave propagation, which are related especially to long transmission lines, can be easily considered. Numerical simulations for an example network are included to prove the value of the results.**

***Index Terms*— Flatness-based control, multiterminal high-voltage direct current transmission (HVDC), power grid, power sharing, travelling waves on transmission lines.**

I. Introduction

ELECTRIC power transmission by means of AC is not feasible for transmission distances larger than 1000 km due to high reactive currents and undesired wave reflections. High-voltage direct current transmission (HVDC) is an efficient alternative to overcome these limitations [1], [2]. The well-established standard configuration of an HVDC system is a peer-to-peer link connecting two conventional AC networks as depicted in Fig. 1. The AC network and the DC link are coupled by a converter terminal equipped with a power converter [3], which works as an inverter or as a rectifier depending on the direction of the power flow.

Although, currently the vast majority of all implemented HVDC systems are in standard peer-to-peer configuration, there has been increasing interest in HVDC networks with more than two converter terminals, the so called multiterminal HVDC [1], [4]–[6]. As a result of the evolving technology for power converters and the increasing exploitation of renewable energy resources such networks have been put into practice, e.g., for offshore wind farms [7]–[9]. A central goal for the control of an HVDC multiterminal network is to keep the power balance between the electrical power fed into and taken from the DC network by the connected converter stations. Simultaneously, one desires to adjust the power distribution between the converter terminals flexibly during the operation of the system. Furthermore, time delays due to traveling waves can become considerable for long transmission distances [6] and should then be considered.

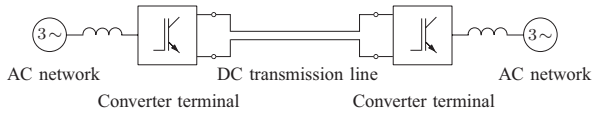

Fig. 1. Peer-to-peer HVDC link with two converter terminals and a DC transmission line connecting them.

This paper proposes a control method that reaches these goals taking a flatness-based approach. For the discussed transmission system, whose description involves partial differential equations (PDEs), this means that the solution of the system equations is parametrized by the trajectories of a special set of system variables, called a flat output of the system [10]–[12]. The number of the components of the flat output equals the number of the control inputs. This contribution recalls the control design approach proposed in [13] and extends it to a more general class of networks.

Section II describes the mathematical model of the HVDC transmission networks investigated. Section III focuses on tree-like, that is cycle-free, networks to explain the derivation of a flat output and the flatness-based control design. The results are illustrated by a numerical example in Section IV. Section V extends the control design approach introduced for tree-like networks to the general network case. This is further clarified in Section VI through a simple example network. Finally, Section VII gives some remarks on practical issues and on potential extensions to be considered for future work.

II. Model of the HVDC Network

This section introduces the mathematical model of the HVDC networks, which the control design is based on.

A. General Network Structure

A general transmission network is assumed to consist of n_P uniquely numbered nodes P_μ, $\mu \in \mathcal{P}$ where $\mathcal{P}$ is the set of all node indices existing in the network. Two arbitrary nodes P_μ and P_ν can be connected by an electric transmission line L_μ^ν where the notations L_μ^ν and L_ν^μ coincide, see Fig. 2.

Manuscript received June 7, 2012; revised October 30, 2012; accepted February 12, 2013. Manuscript received in final form March 14, 2013. Recommended by Associate Editor P. Korba.

C. Schmuck is with the Max Planck Institute for Dynamics of Complex Technical Systems, Magdeburg 39106, Germany, and also with Fachgebiet Regelungssysteme, Technische Universität Berlin, Berlin 10587, Germany (e-mail: schmuck@mpi-magdeburg.mpg.de).

F. Woittennek is with the Institut für Regelungsund Steuerungstheorie, Technische Universität Dresden, Dresden 01187, Germany (e-mail: frank.woittennek@tu-dresden.de).

A. Gensior is with the Professur für Leistungselektronik, Technische Universität Dresden 01187, Germany (e-mail: albrecht.gensior@tu-dresden.de).

J. Rudolph is with the System Theory and Control Engineering, Saarland University, Saarbrücken 66123, Germany (e-mail: j.rudolph@lsr.uni-saarland.de).

Digital Object Identifier 10.1109/TCST.2013.2253322

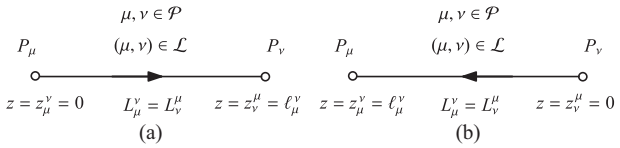

Fig. 2. Nodes and transmission lines in a general network. (a) Notation in case $\mu < \nu$. (b) Notation in case $\mu > \nu$.

Then $\mathcal{L}$ is the set of the index pairs of all n_L existing lines. The spatial variable on the transmission lines is z. On a line L_μ^ν, it takes the value z_μ^ν at node P_μ and the value z_ν^μ at node P_ν, respectively. Furthermore, a direction is assigned to each line from the node with smaller index to the node with greater index. Accordingly, the spatial coordinate values referring to the ends of a line L_μ^ν can be identified as

$$z_\mu^\nu = \begin{cases} 0, & \text{if } \mu < \nu \\ \ell_\mu^\nu, & \text{if } \mu > \nu \end{cases} \tag{1}$$

with $\ell_\mu^\nu = \ell_\nu^\mu$ being the length of line L_μ^ν. Every node P_μ, $\mu \in \mathcal{P}$ can be connected to a converter terminal, which is called C_μ in this case. The set $\mathcal{P}_a \subseteq \mathcal{P}$ comprises the indices of all n_P^a network nodes equipped with a converter terminal, called active nodes, whereas $\mathcal{P}_p = \mathcal{P} \setminus \mathcal{P}_a$ comprises the indices of all $n_P^p = n_P - n_P^a$ nodes without converter terminal, called passive nodes. Every node that is connected to only one line is called terminating node. Obviously, a passive terminating node would be useless in practice, which is why all terminating nodes are assumed to be active.

A node P_μ is called neighbor of node P_ν if there exists a line L_μ^ν, $(\mu, \nu) \in \mathcal{L}$ connecting them. The indices of all m_ν neighbors of P_ν form the set $\mathcal{N}_\nu$.

B. Converter Terminals

Converter terminals are connected to active nodes and form the electric interface between the network and energy sinks, energy sources or neighboring networks.

For each converter terminal C_μ, $\mu \in \mathcal{P}_a$ the voltage is U_μ and the current is I_μ. Because of modern semiconductor technology recent power converters allow to generate almost arbitrary current or voltage trajectories at their DC side [3]. Hence, each converter can be seen either as an ideal current source with a freely adjustable current $I_\mu(t)$ or as an ideal voltage source with a freely adjustable voltage $U_\mu(t)$. The AC part of the converter is therefore neglected. The converters are the actuators of the transmission system. If C_μ is chosen to be a current source then I_μ is a control input of the network. Otherwise, if C_μ is chosen to be a voltage source then U_μ is a control input. The control design is independent from this choice, which thus can be made according to technical aspects.

C. Transmission Line Equations and Boundary Conditions

The model of the transmission lines should allow taking effects such as wave propagation, related delays, and transmission losses into account. Therefore, the voltage profile u_μ^ν and the current profile i_μ^ν on each transmission line L_μ^ν are described by the hyperbolic system of PDEs

$$\frac{\partial u_\mu^\nu}{\partial z}(z,t) + L\frac{\partial i_\mu^\nu}{\partial t}(z,t) + R i_\mu^\nu(z,t) = 0 \tag{2a}$$

$$\frac{\partial i_\mu^\nu}{\partial z}(z,t) + C\frac{\partial u_\mu^\nu}{\partial t}(z,t) + G u_\mu^\nu(z,t) = 0, \quad (\mu,\nu) \in \mathcal{L} \tag{2b}$$

with $z \in (0, \ell_\mu^\nu)$, $t > 0$ and the constant positive, line-specific parameters R, G, L, and C [14]. The notations u_μ^ν and u_ν^μ as well as i_μ^ν and i_ν^μ coincide.

The current i_μ^ν is considered positive in the direction assigned to line L_μ^ν, which is from the node with smaller index to the node with greater index. All voltages are measured with respect to the same common ground reference.

The electrical interconnection of the transmission lines at the network nodes leads to a coupling of the corresponding line PDEs at their boundaries. The boundary conditions result from balancing currents and voltages at each node P_μ. Kirchhoff's current law yields

$$\sum_{k \in \mathcal{N}_\mu} \zeta_\mu^k i_\mu^k(z_\mu^k, t) = \begin{cases} I_\mu(t), & \text{if } \mu \in \mathcal{P}_a \\ 0, & \text{if } \mu \in \mathcal{P}_p \end{cases}, \quad \mu \in \mathcal{P} \tag{3}$$

for the boundary values of the line currents with

$$\zeta_\mu^\nu = \begin{cases} -1 & \text{if } \mu < \nu \\ 1, & \text{if } \mu > \nu \end{cases}$$

accommodating different current orientations. The converter current I_μ is defined to be positive if it is directed away from node P_μ. Moreover, all boundary values of the line voltages at P_μ are equal to the node voltage $\overline{u}_\mu$ at P_μ

$$u_\mu^k(z_\mu^k, t) = \overline{u}_\mu(t), \quad k \in \mathcal{N}_\mu, \quad \mu \in \mathcal{P}. \tag{4a}$$

Accordingly, the voltages at the converters connected to the active nodes of the network are

$$U_\mu(t) = \overline{u}_\mu(t), \quad \mu \in \mathcal{P}_a. \tag{4b}$$

Altogether, the $2n_L$ PDEs (2) and the boundary conditions (3) and (4) constitute a linear distributed parameter model of the transmission network. The currents I_μ or the voltages U_μ, $\mu \in \mathcal{P}_a$ of the converter terminals form the set of n_P^a lumped control inputs located at the boundaries of the transmission lines.

D. Tree-like Networks

A special class of transmission networks are tree-like, that is cycle-free, networks shown in Fig. 3. The absence of transmission line cycles implies that the path between any two converter terminals through the network is unique. Because of this property every node in a tree-like network has a unique predecessor with respect to a certain initial node. Choosing an arbitrary node $P_\alpha, \alpha \in \mathcal{P}$ as this initial node, the predecessor $P_{\rho(\mu)}$ of $P_\mu, \mu \in \mathcal{P} \setminus \{\alpha\}$ is defined as the node that precedes P_μ on the unique path from P_α to P_μ. Note that the predecessor index $\rho(\mu)$ belonging to node P_μ depends on the choice of the initial node P_α although this is not represented by the notation for the sake of simplicity.

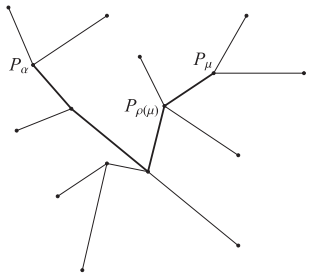

Fig. 3. Network in tree-like structure with an arbitrarily chosen initial node P_α, one of the remaining nodes P_μ and the path between them.

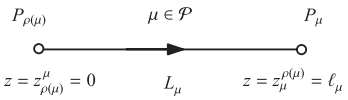

Fig. 4. Simplified notation for nodes and transmission lines in tree-like networks.

Without loss of generality it can be assumed that the nodes along a chosen path are indexed in ascending order such that $\alpha < \rho(\mu) < \mu$. This means, that positive line currents in a chosen path are directed away from the initial node P_α. Then the notation for transmission lines, their node coordinates and their voltage and current profiles may be simplified, see Fig. 4, to

$$L_\mu := L^\mu_{\rho(\mu)} = L^{\rho(\mu)}_\mu, \quad z^\mu_{\rho(\mu)} = 0, \quad z^{\rho(\mu)}_\mu = \ell^{\rho(\mu)}_\mu =: \ell_\mu$$
$$u_\mu := u^{\rho(\mu)}_\mu = u^\mu_{\rho(\mu)}, \quad i_\mu := i^{\rho(\mu)}_\mu = i^\mu_{\rho(\mu)}, \quad \mu \in \mathcal{P} \setminus \{\alpha\}.$$

Regarding the simplified notation and the special role of the initial node P_α, one can reformulate the current boundary conditions (3) to

$$-\sum_{k\in\mathcal{N}_\alpha} i_k(0,t) = \begin{cases} I_\alpha(t), & \text{if } \alpha \in \mathcal{P}_a \\ 0, & \text{if } \alpha \in \mathcal{P}_p \end{cases} \tag{5a}$$

for the initial node P_α see Fig. 5 and

$$i_\mu(\ell_\mu,t) - \sum_{\substack{k\in\mathcal{N}_\mu \\ k\neq\rho(\mu)}} i_k(0,t) = \begin{cases} I_\mu(t), & \mu \in \mathcal{P}_a \setminus \{\alpha\} \\ 0, & \mu \in \mathcal{P}_p \setminus \{\alpha\} \end{cases} \tag{5b}$$

for the remaining node, see Fig. 6. Similarly, the conditions (4) for the voltages can be modified to

$$u_k(0,t) = \overline{u}_\mu(t), \quad k \in \mathcal{N}_\mu \setminus \{\rho(\mu)\}, \quad \mu \in \mathcal{P} \tag{6a}$$
$$u_\mu(\ell_\mu,t) = \overline{u}_\mu(t), \quad \mu \in \mathcal{P} \setminus \{\alpha\} \tag{6b}$$
$$U_\mu(t) = \overline{u}_\mu(t), \quad \mu \in \mathcal{P}_a. \tag{6c}$$

III. Flatness-Based Control Design for Tree-Like Networks

This section introduces the design of a flatness-based feed-forward control. As a first step, only tree-like networks are considered. It is shown that the trajectories of all system variables can be calculated from prescribed trajectories of the current I_α and the voltage U_α of the converter at an arbitrarily chosen initial node P_α and some current allocation parameters (CAPs), which are introduced additionally at each network node. Therefore, the mentioned variables form a flat output of the system. Once the trajectories for the flat output are chosen, the remaining system trajectories can be conveniently calculated from node to node. Finally, this yields the desired control input trajectories for the converter currents or voltages.

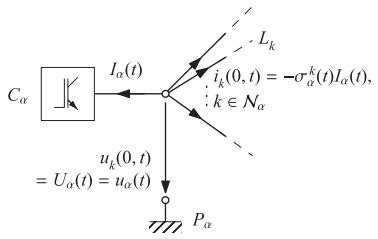

Fig. 5. Currents and voltages at the initial node P_α, $\alpha \in \mathcal{P}_a$ of a tree-like network.

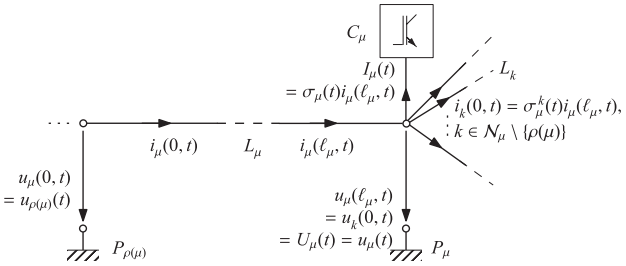

Fig. 6. Currents and voltages at one of the remaining nodes P_μ, $\mu \in \mathcal{P}_a \setminus \{\alpha\}$ and the connected line L_μ in a tree-like network.

A. Derivation of a Flat Output

1) Initial Node: The first step is to choose an arbitrary node with a converter terminal as the initial node P_α, $\alpha \in \mathcal{P}_a$. This determines the simplified notation for the network, which is clarified by Figs. 5 and 6. In the following, the system variables shall be calculated from some prescribed current $I_\alpha(t)$ and voltage $U_\alpha(t)$ at C_α. Because of (6a) and (6c), the converter voltage U_α directly gives the line voltages

$$u_k(0,t) = U_\alpha(t), \quad k \in \mathcal{N}_\alpha \tag{7}$$

of the lines connected at P_α. To determine the currents at P_α one introduces m_α real, time-varying current allocation parameters (CAP) σ^k_α, such that

$$i_k(0,t) = -\sigma^k_\alpha(t) I_\alpha(t), \quad k \in \mathcal{N}_\alpha \tag{8}$$

where

$$\sum_{k\in\mathcal{N}_\alpha} \sigma^k_\alpha(t) = 1 \tag{9}$$

has to be guaranteed to avoid the violation of the current law (5a). This means that the trajectories for $(m_\alpha - 1)$ of the m_α new parameters can be chosen freely to determine the desired fraction (8) of $I_\alpha(t)$ for each line L_k, $k \in \mathcal{N}_\alpha$ at node P_α. The vector comprising these $(m_\alpha - 1)$ chosen parameters as components is denoted by $\boldsymbol{\sigma}_\alpha$ in the following. The equations (7)–(9) give a complete parameterization of the line voltages $u_k(0,t)$ and currents $i_k(0,t)$, $k \in \mathcal{N}_\alpha$ at node P_α in terms of U_α, I_α and $\boldsymbol{\sigma}_\alpha$.

2) Remaining Nodes: Fig. 6 shows one of the remaining network nodes, P_μ, $\mu \in \mathcal{P}\setminus\{\alpha\}$, its unique predecessor $P_{\rho(\mu)}$, and the line L_μ connecting them. The solution of the PDEs (2) allows for the direct calculation of the voltage and current trajectories of line L_μ at P_μ from some known voltage and current trajectories at the preceding end at $P_{\rho(\mu)}$ through

$$\begin{aligned} u_\mu(\ell_\mu,t) &= \frac{e^{-\gamma\tau_\mu}}{2}u_\mu(0,t-\tau_\mu)+\frac{e^{\gamma\tau_\mu}}{2}u_\mu(0,t+\tau_\mu)\\ &\quad+\int_{-\tau_\mu}^{\tau_\mu} g(\ell_\mu,\bar{t})\,u_\mu(0,t-\bar{t})\,\mathrm{d}\bar{t}\\ &\quad+\sqrt{\frac{L}{C}}\Bigg(\frac{e^{-\gamma\tau_\mu}}{2}i_\mu(0,t-\tau_\mu)\\ &\qquad-\frac{e^{\gamma\tau_\mu}}{2}i_\mu(0,t+\tau_\mu)\Bigg)\\ &\quad-\int_{-\tau_\mu}^{\tau_\mu} h_u(\ell_\mu,\bar{t})\,i_\mu(0,t-\bar{t})\,\mathrm{d}\bar{t} \end{aligned} \tag{10a}$$

$$\begin{aligned} i_\mu(\ell_\mu,t) &= \frac{e^{-\gamma\tau_\mu}}{2}i_\mu(0,t-\tau_\mu)+\frac{e^{\gamma\tau_\mu}}{2}i_\mu(0,t+\tau_\mu)\\ &\quad+\int_{-\tau_\mu}^{\tau_\mu} g(\ell_\mu,\bar{t})\,i_\mu(0,t-\bar{t})\,\mathrm{d}\bar{t}\\ &\quad+\sqrt{\frac{C}{L}}\Bigg(\frac{e^{-\gamma\tau_\mu}}{2}u_\mu(0,t-\tau_\mu)\\ &\qquad-\frac{e^{\gamma\tau_\mu}}{2}u_\mu(0,t+\tau_\mu)\Bigg)\\ &\quad-\int_{-\tau_\mu}^{\tau_\mu} h_i(\ell_\mu,\bar{t})\,u_\mu(0,t-\bar{t})\,\mathrm{d}\bar{t} \end{aligned} \tag{10b}$$

with $\epsilon=\sqrt{LC}$, $\tau_\mu=\epsilon\ell_\mu$ and the functions

$$\begin{aligned} h_u(z,t) &= Rf(z,t)+L\frac{\partial f}{\partial t}(z,t)\\ h_i(z,t) &= Gf(z,t)+C\frac{\partial f}{\partial t}(z,t)\\ g(z,t) &= \frac{\partial f}{\partial z}(z,t)\\ f(z,t) &= \frac{e^{-\gamma t}}{2\epsilon}J_0(\beta\sqrt{\epsilon^2z^2-t^2}) \end{aligned}$$

employing the Bessel function J_0 of the first kind and the constants

$$\beta=\frac{1}{2}\left(\frac{R}{L}-\frac{G}{C}\right),\quad \gamma=\frac{1}{2}\left(\frac{R}{L}+\frac{G}{C}\right)$$

see [15]. Equations (10) reflect the wave propagation process taking place on line L_μ as they involve distributed delays and predictions. Thus the values $u_\mu(\ell_\mu,t)$ and $i_\mu(\ell_\mu,t)$ at a certain time instant t are determined by the trajectories of $u_\mu(0,\bar{t})$ and $i_\mu(0,\bar{t})$ on the complete time interval $\bar{t}\in[t-\tau_\mu,t+\tau_\mu]$. The delay τ_μ can be interpreted as the time that a voltage and current wave needs to travel between the ends of the line L_μ.

Analogously to the procedure at the initial node, the distribution of the currents between the lines and a possibly connected converter at P_μ shall be determined by $(m_\mu-1)$ CAPs σ_μ^k, $k\in\mathcal{N}_\mu\setminus\{\rho(\mu)\}$ and an additional CAP $\overline{\sigma}_\mu$ if P_μ is active. Thus

$$i_k(0,t)=\sigma_\mu^k(t)\,i_\mu(\ell_\mu,t),\quad k\in\mathcal{N}_\mu\setminus\{\rho(\mu)\} \tag{11a}$$

$$I_\mu(t)=\overline{\sigma}_\mu(t)\,i_\mu(\ell_\mu,t),\quad \text{if } \mu\in\mathcal{P}_a. \tag{11b}$$

Again Kirchhoff's current law (5b) requires

$$\sum_{\substack{k\in\mathcal{N}_\mu\\ k\neq\rho(\mu)}}\sigma_\mu^k(t)=\begin{cases}1, & \text{if } \mu\in\mathcal{P}_p\\ 1-\overline{\sigma}_\mu(t), & \text{if } \mu\in\mathcal{P}_a\end{cases} \tag{12}$$

by which one can freely choose the trajectories for only $(m_\mu-2)$ out of $(m_\mu-1)$ CAPs if $\mu\in\mathcal{P}_p$ or $(m_\mu-1)$ out of m_μ CAPs if $\mu\in\mathcal{P}_a$. The vector comprising these chosen parameters as components is denoted by $\boldsymbol{\sigma}_\mu$. According to (6), the voltages at P_μ are

$$u_k(0,t)=\overline{u}_\mu(t)=u_\mu(\ell_\mu,t),\quad k\in\mathcal{N}_\mu\setminus\{\rho(\mu)\} \tag{13a}$$

$$U_\mu(t)=u_\mu(\ell_\mu,t),\quad \text{if } \mu\in\mathcal{P}_a. \tag{13b}$$

Equations (10)–(13) give a parameterization of all voltages and currents at P_μ in terms of the voltage $u_\mu(0,t)$ and the current $i_\mu(0,t)$ at the preceding node $P_{\rho(\mu)}$ and the CAPs $\boldsymbol{\sigma}_\mu$ at P_μ. These equations hold for all remaining nodes P_μ, $\mu\in\mathcal{P}\setminus\{\alpha\}$. Therefore, it is now possible to calculate all voltage and current trajectories at each node in the network from the trajectories of U_α and I_α at the initial node and the freely determined CAP trajectories $\boldsymbol{\sigma}_\mu$, $\mu\in\mathcal{P}$ at the network nodes. Hence, these variables form the flat output

$$\boldsymbol{y}=\left(U_\alpha,I_\alpha,(\boldsymbol{\sigma}_\mu)_{\mu\in\mathcal{P}}\right) \tag{14}$$

of the transmission network.

Clearly, it is convenient to perform the calculations of the system trajectories stepwise from node to node beginning at the initial node P_α. Firstly, (7) and (8) are used to determine the voltage and current trajectories at node P_α from the determined trajectories of U_α, I_α and the chosen CAPs $\boldsymbol{\sigma}_\alpha$. Then, the neighbors of P_α are considered. Their predecessor is P_α. Employing (10)–(13) with $\rho(\mu)=\alpha$ together with the CAP trajectories for each node P_μ, $\mu\in\mathcal{N}_\alpha$ gives all voltage and current trajectories at these nodes. In the next step, these nodes P_μ serve as predecessors for all their neighbors (except P_α) and (10)–(13) can be applied again. One follows this procedure until finally all terminating nodes are reached. A particular result of these calculations are the trajectories of the converter currents I_μ and voltages U_μ, $\mu\in\mathcal{P}_a$ obtained in (11b) and (13b). Together with the trajectories for I_α and U_α, these are the feed-forward control trajectories that will lead to the system behavior defined by the previously chosen trajectories for the flat output.

Note that the initial node plays a special role in the operation of the network. In contrast to the other nodes, the converter current and voltage trajectories at this node can be chosen freely as they are included in the flat output $\boldsymbol{y}$. Therefore, if a direct determination of the current or voltage trajectories at a certain node is desired for some operational maneuver this node should be chosen as the initial node. It might be useful to choose different initial nodes for different maneuvers. The CAPs being the remaining components of the flat output $\boldsymbol{y}$ determine the current fractions on the transmission lines at each node. As a result, they can be used to adjust the power distribution between the converter stations within the network.

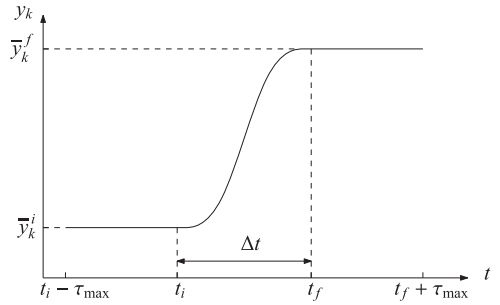

Fig. 7. Polynomial trajectory for one component y_k of the flat output $\boldsymbol{y}$ during the transition between two states of rest according to (16).

B. Trajectory Planning: Transition Between Two States of Rest

Several control tasks can be solved much easier if a flat output of the system is known. A particular example is the transition between two states of rest, which is relevant for the application of this paper as well. Most of the time the HVDC system will be operated in a balanced state of rest with constant voltage and current values, which meet all operational requirements. If these requirements change, the transition to a suitable new state of rest will be desired.

In a state of rest, every system variable remains constant over time by definition. As for flat systems all trajectories are parameterized by the flat output and its derivatives, each state of rest of the system is completely characterized by constant values $\overline{y}_k$ for the n_y components y_k, $k = 1, 2, \ldots, n_y$ of the flat output

$$y_k(t) = \overline{y}_k, \quad \frac{d^j y_k(t)}{dt^j} = 0, \quad j = 1, 2, \ldots \tag{15}$$

To implement the transition from an initial state of rest with $y_k(t) = \overline{y}_k^i$ to a new final state of rest with $y_k(t) = \overline{y}_k^f$ one can choose polynomials $p_k(t)$ to connect the constant parts of the trajectories, such that

$$y_k(t) = \begin{cases} \overline{y}_k^i, & \text{if } t < t_i \\ p_k(t), & \text{if } t_i \le t \le t_f \\ \overline{y}_k^f, & \text{if } t > t_f \end{cases} \tag{16}$$

with

$$p_k(t_i) = \overline{y}_k^i, \quad p_k(t_f) = \overline{y}_k^f \tag{17a}$$

$$\frac{dp_k}{dt}(t_i) = 0, \quad \frac{dp_k}{dt}(t_f) = 0, \quad k = 1, 2, \ldots, n_y. \tag{17b}$$

The obtained trajectory for one component y_k is depicted in Fig. 7. The desired transition time $\Delta t = t_f - t_i$ can be chosen freely.

The conditions (17b) assure continuous differentiability with respect to time for the trajectories of the flat output. This smoothness is maintained during the computations in Section III-A as differentiations with respect to time do not occur. Thus, continuous differentiability is obtained for all system trajectories. The four requirements of (17) can be met with the polynomials of degree three

$$p_k(t) = \overline{y}_k^i + \left(\overline{y}_k^f - \overline{y}_k^i\right)\left(3 - 2t_*\right)t_*^2, \quad t_* = \frac{t - t_i}{t_f - t_i}$$
$$k = 1, 2, \ldots, n_y. \tag{18}$$

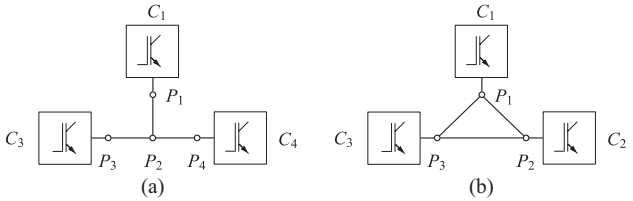

Fig. 8. Simple example networks with three converters. (a) Tree-like case. (b) General case with a line cycle.

The subsequent computation of the remaining system trajectories according to the stepwise procedure of Section III comprises the repeated use of (10) including predictions and delays. This entails that the chosen trajectories (16) are involved on some larger time interval[1] $[t_i - \tau_{\max}, t_f + \tau_{\max}]$ rather than only on $[t_i, t_f]$ as indicated in Fig. 7. The resulting system trajectories and the control input trajectories in particular will leave their initial constant values already up to $\tau_{\max}$ before $t = t_i$ and they will reach their final constant values up to $\tau_{\max}$ after $t = t_f$. Again, this reflects the wave propagation process taking place on the transmission lines. In practice, this means that an operational maneuver, which intends to change the values of the variables belonging to the flat output $\boldsymbol{y}$ within $t_i \le t \le t_f$, has to start at $t = t_i - \tau_{\max}$ and will not end before $t = t_f + \tau_{\max}$.

IV. Simple Tree-Like Example Network

The results from Section III shall now be illustrated with the help of a simple example network with $n_P = 4$ nodes and $n_L = 3$ transmission lines as shown in Fig. 8(a). The network is specified by the sets

$$\mathcal{P} = \{1, 2, 3, 4\}, \quad \mathcal{P}_a = \{1, 3, 4\}, \quad \mathcal{P}_p = \{2\}$$
$$\mathcal{L} = \{(1, 2), (2, 3), (2, 4)\}$$
$$\mathcal{N}_1 = \mathcal{N}_3 = \mathcal{N}_4 = \{2\}, \quad \mathcal{N}_2 = \{1, 3, 4\}.$$

Hence, the control inputs of the system are the currents or the voltages of the three converters.

It is assumed that the converter current I_1 is required to change from an initial value of 0 to a new constant desired value I_d while the converter voltage U_1 remains at a constant value U_d. As the voltage and current values at converter C_1 shall be determined node, P_1 is chosen as initial node. This yields the notation shown in Fig. 9 and the network-specific values $\alpha = 1$, $\rho(2) = 1$, $\rho(3) = 2$, and $\rho(4) = 2$.

A. Flat Output

The stepwise procedure from Section III-A adapts to this example network as follows. According to (14) the first two components of the flat output $\boldsymbol{y}$ are U_1 and I_1. The currents and voltages at P_1

$$u_2(0, t) = U_1(t), \quad i_2(0, t) = -I_1(t) \tag{19}$$

[1]The maximum delay time $\tau_{\max}$ can be computed by $\tau_{\max} = \max_{k \in \mathcal{P}_t} \tilde{\tau}_k$ where $\mathcal{P}_t$ is the set of the indices of all terminating nodes of the network and $\tilde{\tau}_\mu$ the sum of all delays τ_k of the lines L_k forming the path from the initial node P_α to the terminating node P_μ, $\mu \in \mathcal{P}_t$. This means $\tilde{\tau}_\mu$ is the time that a current and voltage wave needs to travel from the initial node P_α to the terminating node P_μ.

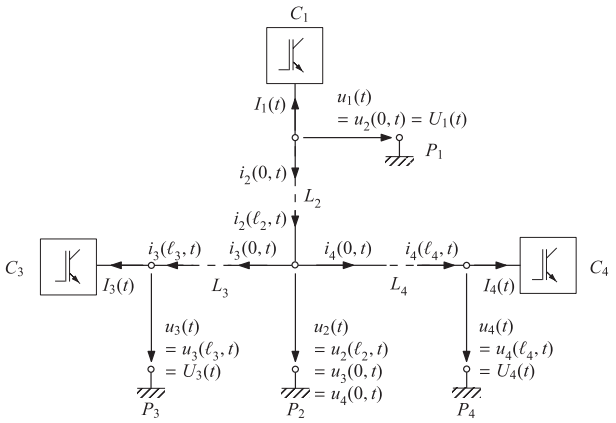

Fig. 9. Tree-like network with three converters and the notation for the case of P_1 being chosen as initial node.

are obtained using (7) and (8). No CAP is introduced at P_1 as only one transmission line is connected ($m_1 = 1$). Proceeding to the only neighbor of P_1, which is P_2, equations (10) with $\mu = 2$ and $\rho(\mu) = 1$ allow to compute $u_2(\ell_2, t)$ and $i_2(\ell_2, t)$ from $u_2(0, t)$ and $i_2(0, t)$. As $m_2 = 3$ lines are connected to the passive node P_2, one needs to introduce $m_2 - 1 = 2$ CAPs ${\sigma_2}^3$, ${\sigma_2}^4$ to determine the currents and voltages

$$u_k(0,t) = u_2(\ell_2,t), \quad i_k(0,t) = {\sigma_2}^k(t) i_2(\ell_2,t), \qquad k = 3,4 \tag{20}$$

according to (11a) and (13a). The trajectory for only $m_2 - 2 = 1$ of the two CAPs ${\sigma_2}^3$, ${\sigma_2}^4$ can be chosen freely. For this example, ${\sigma_2}^3$ is selected and is therefore included in the flat output as the third component. After that, the other CAP is determined by (12) as

$${\sigma_2}^4(t) = 1 - {\sigma_2}^3(t). \tag{21}$$

Now the last two nodes can be considered. Employing (10) with $\mu = 3$, $\rho(\mu) = 2$ for line L_3 and again with $\mu = 4$, $\rho(\mu) = 2$ for line L_4 yields $u_k(\ell_k, t)$, $i_k(\ell_k, t)$, $k = 3, 4$. Then the voltages and currents at the converters C_3 and C_4 follow from (11b)

$$U_k(t) = u_k(\ell_k,t), \quad I_k(t) = i_k(\ell_k,t) \qquad k = 3,4. \tag{22}$$

At the nodes P_3 and P_4, again no new CAPs are introduced since there is only one line per node ($m_3 = m_4 = 1$). Finally, all system variables are calculated and the flat output of the example network is

$$\boldsymbol{y} = \left(U_1, I_1, {\sigma_2}^3\right). \tag{23}$$

B. Trajectory Planning

Apart from the variables U_1 and I_1, the trajectory for the third component ${\sigma_2}^3$ of $\boldsymbol{y}$ can be prescribed freely as well. It determines how the line current $i_2(\ell_2, t)$ is split between line L_3 and line L_4, and it can hence be exploited to set the power distribution between the converters C_3 and C_4. For the sake of simplicity, ${\sigma_2}^3$ shall remain at a constant value of 0.3 during the maneuver to be planned. The two states of rest corresponding to the required current change at C_1 with constant current voltage U_1 and CAP ${\sigma_2}^3$ are characterized by

$$\begin{aligned} {\overline{y}_1}^i &= U_d, \quad {\overline{y}_2}^i = 0, \quad {\overline{y}_3}^i = 0.3 \\ {\overline{y}_1}^f &= U_d, \quad {\overline{y}_2}^f = I_d, \quad {\overline{y}_3}^f = 0.3. \end{aligned}$$

If the suggested polynomial trajectories (16) with an arbitrarily fixed transition time Δt are now assigned to the variables of the flat output, all remaining system trajectories can be computed using the procedure described in Section IV-A. In (22), this yields particularly the desired converter current and voltage trajectories. For each of the three converters, one may choose either its current or its voltage as control input according to the technical realities of the converter stations. If the calculated converter trajectories are applied to the system, it will show the behavior predefined by the trajectories of the flat output.

To illustrate the results, the system trajectories are computed using a set of numerical parameter values given in Table I. The resulting trajectories in Fig. 10 clarify that the transition of the complete system between the two states of rest takes longer than only the prescribed transition time $\Delta t = 5$ ms. The maneuver, which was planned to change I_1 within $t_i \le t \le t_f$, is required to start already at $t = t_i - \tau_{\max} = -20.76$ ms at converter C_4 and ends not before $t = t_f + \tau_{\max} = 25.76$ ms at C_4.[2] The impact of the CAP ${\sigma_2}^3$ is clarified by the dashed graphs in Fig. 10(a). It can be seen that the currents $i_3(0, t)$ and $i_4(0, t)$ are proportional to $i_2(\ell_2, t)$ according to the prescribed constant value ${\sigma_2}^3(t) = 0.3$.

TABLE I
NUMERICAL PARAMETER VALUES

Parameter	Value	Parameter	Value
R	$1 \cdot 10^{-5}\ \Omega\mathrm{m}^{-1}$	$\tau_2 = \epsilon \ell_2$	12.25 ms
G	$3 \cdot 10^{-10}\ \mathrm{Sm}^{-1}$	$\tau_3 = \epsilon \ell_3$	6.12 ms
L	$5 \cdot 10^{-7}\ \mathrm{Hm}^{-1}$	$\tau_4 = \epsilon \ell_4$	8.51 ms
C	$2 \cdot 10^{-10}\ \mathrm{Fm}^{-1}$	$\tau_{\max} = \tau_2 + \tau_4$	20.76 ms
ℓ_2	1000 km	t_i	0 ms
ℓ_3	500 km	Δt	5 ms
ℓ_4	700 km	$t_f = t_i + \Delta t$	5 ms

V. EXTENSION TO GENERAL NETWORKS

For a general network with line cycles, the useful property of unique paths between a pair of nodes is not given anymore. Hence, it cannot be exploited for the retrieval of a flat output and the stepwise calculation of the control input trajectories. To investigate the flatness-based control design for this less convenient case, the system equations are analyzed in the Laplace domain.

[2]The maximum delay time $\tau_{\max}$ given in Table I is the maximum of the two sums $\tau_2 + \tau_3$ and $\tau_2 + \tau_4$, which refer to the travel time of a voltage and current wave from P_1 to P_3 and to P_4, respectively.

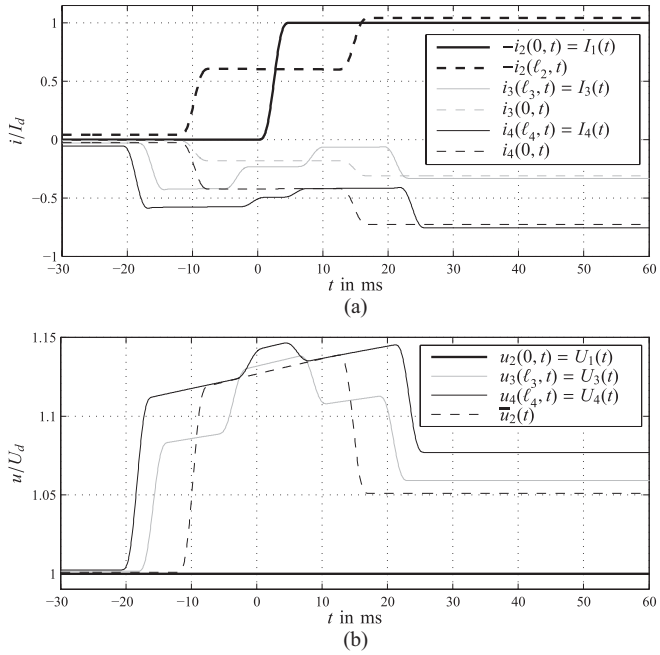

Fig. 10. Current and voltage trajectories for the three lines and converters during the transition between two states of rest for a change of the converter current I_1 at converter C_1 from the initial value $\overline{y}_2^i = 0$ to $\overline{y}_2^f = I_d$ via a polynomial trajectory on $0 \le t \le \Delta t = 5$ ms. (a) Currents at the active nodes (solid line) and at P_2 (dashed line). (b) Node voltages at the active nodes (solid line) and at P_2 (dashed line).

A. System Equations in the Laplace Domain

Laplace transformation[3] renders the line PDEs (2) into first-order ordinary differential equations (ODEs) in z with the solution

$$\begin{pmatrix} \hat{u}_\mu^\nu(z) \\ \hat{i}_\mu^\nu(z) \end{pmatrix} = \Phi(z - z_\mu^\nu) \begin{pmatrix} \hat{u}_\mu^\nu(z_\mu^\nu) \\ \hat{i}_\mu^\nu(z_\mu^\nu) \end{pmatrix}, \quad z \in (0, \ell_\mu^\nu), \quad (\mu,\nu) \in \mathcal{L} \tag{24}$$

describing the current and the voltage on the transmission lines, where

$$\begin{aligned} \Phi(z) &= \begin{pmatrix} K_1(z) & -(G+sC)K_2(z) \\ -(R+sL)K_2(z) & K_1(z) \end{pmatrix} \\ K_1(z) &= \cosh(\lambda z) \\ K_2(z) &= \frac{\sinh(\lambda z)}{\lambda} \\ \lambda &= \sqrt{RG + s(RC+LG) + s^2 LC}. \end{aligned}$$

Evaluating (24) at the boundary $z = z_\nu^\mu$ together with (1) and the boundary conditions (4a) leads to

$$\begin{pmatrix} \hat{\overline{u}}_\mu \\ \hat{i}_\mu^\nu(z_\nu^\mu) \end{pmatrix} = \Phi(-\zeta_\mu^\nu \ell_\mu^\nu) \begin{pmatrix} \hat{\overline{u}}_\nu \\ \hat{i}_\mu^\nu(z_\mu^\nu) \end{pmatrix}, \quad (\mu,\nu) \in \mathcal{L}. \tag{25}$$

After replacing the node voltages $\hat{\overline{u}}_\mu$ at each active node according to (4b) by the converter voltages $\hat{U}_\mu$ (25) gives $2n_L$ equations for n_P^p node voltages, n_P^a converter voltages and $2n_L$ currents at the boundaries of the lines. The boundary conditions (3) give a further set of n_P equations

$$\sum_{k \in \mathcal{N}_\mu} \zeta_\mu^k \hat{i}_\mu^k(z_\mu^k) = \begin{cases} \hat{I}_\mu, & \text{if } \mu \in \mathcal{P}_a \\ 0, & \text{if } \mu \in \mathcal{P}_p \end{cases}, \quad \mu \in \mathcal{P} \tag{26}$$

and introduce the n_P^a existing converter currents. In total, (25) and (26) form a system Σ of $2n_L + n_P$ equations, which are linear in the $2n_L + n_P^p + 2n_P^a = 2n_L + n_P + n_P^a$ variables

$$\left(\left(\hat{i}_\mu^\nu(z_\mu^\nu), \hat{i}_\mu^\nu(z_\nu^\mu) \right)_{(\mu,\nu)\in\mathcal{L}}, (\hat{\overline{u}}_\mu)_{\mu\in\mathcal{P}_p}, (\hat{I}_\mu, \hat{U}_\mu)_{\mu\in\mathcal{P}_a} \right). \tag{27}$$

Thus, in accordance with the number of control inputs, n_P^a variables can be chosen freely.[4]

B. Flat Output

A flat output for the system Σ can be found as follows [10]–[12]. One chooses n_P^a variables from (27) to constitute the vector $\hat{\boldsymbol{v}}$. The remaining $2n_L + n_P$ variables are merged in the vector $\hat{\boldsymbol{x}}$ such that the equations of system Σ can be written in the form $D\hat{\boldsymbol{x}} = Q\hat{\boldsymbol{v}}$ with a quadratic matrix D. The variables for $\hat{\boldsymbol{v}}$ have to be chosen in a way that guarantees $\det(D)|_{s=0} \neq 0$. Then, by

$$\hat{\boldsymbol{v}} = \det(D)\hat{\boldsymbol{y}}, \quad \hat{\boldsymbol{x}} = \operatorname{adj}(D) Q \hat{\boldsymbol{y}} \tag{28}$$

a flat output $\hat{\boldsymbol{y}}$ can be introduced.[5] The elements of $\hat{\boldsymbol{y}}$ are independent and parameterize all system variables $\hat{\boldsymbol{v}}$ and $\hat{\boldsymbol{x}}$. Obviously, the elements of $\boldsymbol{y}$ do not necessarily coincide directly with system variables anymore in the general network case. However, the system variables $\boldsymbol{v}$ play a special role since they differ from the flat output only by the scalar factor $\det(D)$ in the Laplace domain. Hence, operational demands on $\boldsymbol{v}$, e.g., desired steady-state values, can be easily fulfilled by appropriate trajectory planning for $\boldsymbol{y}$. This should be kept in mind when choosing the elements of $\hat{\boldsymbol{v}}$.

C. Trajectory Planning

Similar to the case of tree-like networks, the trajectories of $\boldsymbol{y}$ can be prescribed freely to implement, e.g., a transition between two states of rest of the system. Some given desired initial and final steady-state values $\overline{v}_k^i$ and $\overline{v}_k^f$, $k = 1, \ldots, n_P^a$ for the components of $\boldsymbol{v}$ can be translated into corresponding values of the flat output by

$$\overline{y}_k^j = \frac{\overline{v}_k^j}{\det(D)|_{s=0}}, \quad k = 1, \ldots, n_P^a, \quad j \in \{i, f\} \tag{29}$$

employing (28) with $s = 0$. Again, polynomial trajectories of the form (16) might be used for the flat output to connect the two states of rest. From these trajectories, the trajectories for all system variables $\boldsymbol{x}$ and $\boldsymbol{v}$, especially the desired control inputs, can be calculated with the help of

[3] In the following, the Laplace transform of a quantity x is denoted by $\hat{x}$ and the Laplace variable is s.

[4] The variables (27) do not include any CAPs as introduced in Section III-A. However, a CAP can be seen as a fraction of two currents at one of the network nodes. Hence, CAPs could be introduced as alternative degrees of freedom for general networks as well.

[5] Strictly speaking, the quantity $\boldsymbol{y}$ does not satisfy the rigorous definition of a flat output. However, the details are not relevant for the application above. Thus, the term "flat output" is used although this is a slight abuse of terminology.

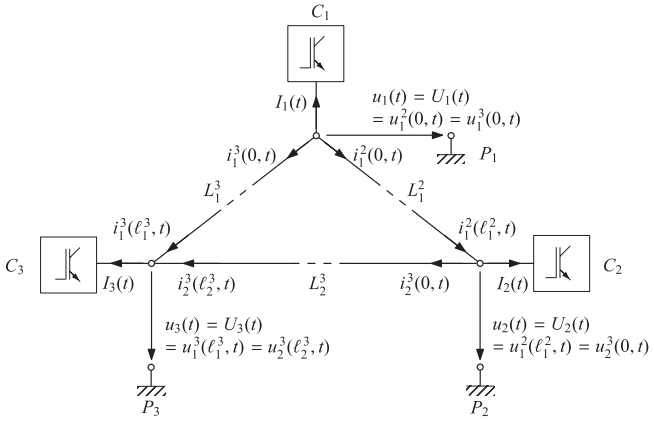

Fig. 11. General network involving three converters and a line cycle with currents and voltages at each node.

(28). This replaces the stepwise calculation procedure for tree-like networks described in Section III-A. For this purpose, (28) has to be transformed back into the time domain using the relations

$$K_2(z)\hat{u} \triangleq \int_{-z\epsilon}^{z\epsilon} f(z,\overline{t}\,)u(t-\overline{t}\,)\,\mathrm{d}\overline{t} \tag{30a}$$

$$K_1(z)\hat{u} \triangleq \int_{-z\epsilon}^{z\epsilon} \frac{\partial f}{\partial z}(z,\overline{t}\,)u(t-\overline{t}\,)\,\mathrm{d}\overline{t} + \epsilon\,(f(z,z\epsilon)u(t-z\epsilon) + f(z,-z\epsilon)u(t+z\epsilon)) \tag{30b}$$

$$sK_2(z)\hat{u} \triangleq \int_{-z\epsilon}^{z\epsilon} \frac{\partial f}{\partial \overline{t}}(z,\overline{t}\,)u(t-\overline{t}\,)\,\mathrm{d}\overline{t} + f(z,-z\epsilon)u(t+z\epsilon) - f(z,z\epsilon)u(t-z\epsilon) \tag{30c}$$

which again involve distributed delays and predictions similar to (10).

VI. Simple Example for the General Case

To illustrate the results of Section V, the example network sketched in Figs. 8(b) and 11 is considered. It consists of $n_P = 3$ nodes, $n_L = 3$ lines and $n_P^a = 3$ converters and it is characterized by the sets

$$\mathcal{P} = \{1,2,3\},\quad \mathcal{N}_1 = \{2,3\},\quad \mathcal{N}_2 = \{1,3\},\quad \mathcal{N}_3 = \{1,2\}$$
$$\mathcal{P}_a = \{1,2,3\},\quad \mathcal{P}_p = \emptyset,\quad \mathcal{L} = \{(1,2),(2,3),(1,3)\}.$$

The spatial coordinates are

$$z_1^2 = 0,\quad z_1^3 = 0,\quad z_2^3 = 0,\quad z_2^1 = \ell_1^2,\quad z_3^1 = \ell_1^3,\quad z_3^2 = \ell_2^3.$$

According to the number of converters the vector $\hat{\boldsymbol{v}}$ as well as the flat output must have $n_P^a = 3$ components. In total, (25) and (26) give 9 equations for the 12 variables (27). Now it is exemplarily assumed that the steady-state values of the variables U_3, I_1 and I_2 are required to be changed to a new value within an operational maneuver. This suggests $\hat{\boldsymbol{v}} = (\hat{U}_3\ \hat{I}_1\ \hat{I}_2)^T$, which implies the system representation $D\hat{\boldsymbol{x}} = Q\hat{\boldsymbol{v}}$ with $\hat{\boldsymbol{x}}$, Q and D, as shown in the equations at the bottom of the page, and $\Phi_{12}(z) = -(G+sC)K_2(z)$, $\Phi_{21}(z) = -(R+sL)K_2(z)$, such that

$$\det(D) = (G+sC)K_2(\ell_1^2 + \ell_1^3 + \ell_2^3).$$

According to (28), a flat output $\hat{\boldsymbol{y}}$ can now be introduced by

$$\hat{\boldsymbol{v}} = (G+sC)K_2(\ell_1^2 + \ell_1^3 + \ell_2^3)\hat{\boldsymbol{y}},\quad \hat{\boldsymbol{x}} = \mathrm{adj}(D)Q\hat{\boldsymbol{y}}. \tag{31}$$

To implement the desired transition from some initial values $\overline{v}_k^i$ to some final values $\overline{v}_k^f$, $k = 1,\ldots,n_P^a$ appropriate trajectories for $\boldsymbol{y}$ have to be planned. Because of (29) and

$$\det(D)|_{s=0} = \sqrt{G/R}\sinh\left(\sqrt{RG}(\ell_1^2 + \ell_1^3 + \ell_2^3)\right)$$

the relevant steady-state values $\overline{y}_k^i$ and $\overline{y}_k^f$ to be smoothly connected by the trajectories of $\boldsymbol{y}$ are

$$\overline{y}_k^j = \frac{\overline{v}_k^j}{\sqrt{G/R}\sinh\left(\sqrt{RG}(\ell_1^2 + \ell_1^3 + \ell_2^3)\right)}$$

$k = 1,\ldots,n_P^a$, $j \in \{i,f\}$. Then the trajectories of the remaining system variables are computed with the help of (31) and (30a)

$$\boldsymbol{v}(t) = \int_{-(\ell_1^2+\ell_1^3+\ell_2^3)\epsilon}^{(\ell_1^2+\ell_1^3+\ell_2^3)\epsilon} f(z,\overline{t}\,)(G\boldsymbol{y}(t-\overline{t}\,) + C\dot{\boldsymbol{y}}(t-\overline{t}\,))\,\mathrm{d}\overline{t}. \tag{32}$$

$$\hat{\boldsymbol{x}} = \begin{pmatrix}\hat{U}_1 & \hat{U}_2 & \hat{I}_3 & \hat{i}_1^2(0) & \hat{i}_1^3(0) & \hat{i}_2^3(0) & \hat{i}_1^2(\ell_1^2) & \hat{i}_1^3(\ell_1^3) & \hat{i}_2^3(\ell_2^3)\end{pmatrix}^T$$

$$Q = \begin{pmatrix}0&0&0&0&1&1&0&0&0\\1&0&0&0&0&0&0&0&0\\0&1&0&0&0&0&0&0&0\end{pmatrix}^T$$

$$D = \begin{pmatrix}
0 & 0 & 0 & -1 & -1 & 0 & 0 & 0 & 0\\
0 & 0 & 0 & 0 & 0 & -1 & 1 & 0 & 0\\
0 & 0 & 1 & 0 & 0 & 0 & 0 & 1 & 1\\
C_1(\ell_1^2) & -1 & 0 & \Phi_{12}(\ell_1^2) & 0 & 0 & 0 & 0 & 0\\
C_1(\ell_1^3) & 0 & 0 & 0 & \Phi_{12}(\ell_1^3) & 0 & 0 & 0 & 0\\
0 & C_1(\ell_2^3) & 0 & 0 & 0 & \Phi_{12}(\ell_2^3) & 0 & 0 & 0\\
\Phi_{21}(\ell_1^2) & 0 & 0 & C_1(\ell_1^2) & 0 & 0 & -1 & 0 & 0\\
\Phi_{21}(\ell_1^3) & 0 & 0 & 0 & C_1(\ell_1^3) & 0 & 0 & -1 & 0\\
0 & \Phi_{21}(\ell_2^3) & 0 & 0 & 0 & C_1(\ell_2^3) & 0 & 0 & -1
\end{pmatrix}$$

For the sake of brevity, the equations for $\boldsymbol{x}(t)$ are not given here explicitly. The vectors $\boldsymbol{v}(t)$ and $\boldsymbol{x}(t)$ include the three control input signals, which are either $U_\mu(t)$ or $I_\mu(t)$ at each converter C_μ, $\mu = 1, 2, 3$. Applying these input signals will effect the transfer between two states of rest as parameterized by the prescribed trajectories for the flat output. The result (32) shows that this maneuver extends to the interval $[t_i - \tau_{\max}, t_f + \tau_{\max}]$ with $\tau_{\max} = (\ell_1^2 + \ell_1^3 + \ell_2^3)\epsilon$ when the flat output is planned to transfer within $[t_i, t_f]$ according to (16). Similar to the tree-like case described in Section III-B, this reflects the predictions and delays due to the consideration of wave propagation processes.

VII. Further Remarks and Future Work

The converter terminals connected to the network were modeled as ideal current or voltage sources—see Section II-B–to yield a comprehensible presentation of the proposed control method. In practical applications, the specific capabilities of the converter devices and the characteristics of the connected AC side that have been neglected with the idealized converter model might possibly limit admissible trajectories in the network. However, this did not restrict the use of the control method as such limits can be fully taken into account by planning the trajectories for the flat output appropriately.

If a flat output and a certain trajectory form [e.g., (16)] is fixed, the resulting system trajectories for different trajectory planning procedures will differ only in a few parameters but not in their form. Thus, the complete calculations of Section III-A, or V-C, respectively, need to be performed only once for the first planning procedure. For following maneuvers only the trajectory parameters have to be updated. This reduces the computational effort considerably.

The control scheme suggested is particularly useful for HVDC networks with long transmission lines as wave propagation processes and related delays are considered. However, it can be also applied to systems with transmission lines short enough to neglect delays still providing a powerful tool for planning load change maneuvers and power sharing. In this case, each transmission line might be modeled by a network of lumped RLC-elements such that the line PDEs (2) are replaced by ODEs in t. This does not preclude the proposed design approach. As the new line equations do not model wave propagation anymore, no delays and predictions will occur in the calculations of the system trajectories. As a result, all system variables will transfer between their steady-state values within the same time interval $[t_i, t_f]$ as the flat output and the total duration of a planned maneuver will reduce to $\Delta t = t_i - t_f$.

To face the problem of model uncertainties and disturbances, the feed-forward control scheme could be extended by local feed-back controllers at each converter. This is a potential topic for future work.

References

[1] J. Arrillaga, *High Voltage Direct Current Transmission* (Power and Energy Series), vol. 29. New York, NY, USA: The Institution of Electrical Engineers, 1998.

[2] E. Peschke and R. V. Olshausen, *Kabelanlagen für Hoch- und Höchstspannung*. Munich, Germany: Publicis-MCD-Verlag, 1998.

[3] N. Mohan, T. Undeland, and W. Robbins, *Power Electronics*. New York, NY, USA: Wiley, 2002.

[4] P. Karlson, "DC distributed power systems—analysis, design and control for a renewable energy system," Ph.D. dissertation, Dept. Ind. Electr. Eng. Autom., Lund Univ., Lund, Sweden, 2002.

[5] H. Jiang and A. Ekstrom, "Multiterminal HVDC systems in urban areas of large cities," *IEEE Trans. Power Del.*, vol. 13, no. 4, pp. 1278–1284, Oct. 1998.

[6] V. Lescale, A. Kumar, L.-E. Juhlin, H. Bjorklund, and K. Nyberg, "Challenges with multi-terminal UHVDC transmissions," in *Proc. Joint Int. Conf. Power Syst. Technol., IEEE Power India Conf.*, Oct. 2008, pp. 1–7.

[7] L. Jun, O. Gomis-Bellmunt, J. Ekanayake, and N. Jenkins, "Control of multi-terminal VSC-HVDC transmission for offshore wind power," in *Proc. 13th Eur. Conf. Power Electron. Appl.*, Sep. 2009, pp. 1–10.

[8] L. Xu and L. Yao, "DC voltage control and power dispatch of a multi-terminal HVDC system for integrating large offshore wind farms," *Renew. Power Generat., IET*, vol. 5, no. 3, pp. 223–233, May 2011.

[9] W. Lu and B. Ooi, "Optimal acquisition and aggregation of offshore wind power by multiterminal voltage-source HVDC," *IEEE Power Eng. Rev.*, vol. 22, no. 8, pp. 71–72, Aug. 2002.

[10] J. Rudolph and F. Woittennek, "Motion planning and open loop control design for linear distributed parameter systems with lumped controls," *Int. J. Control*, vol. 81, no. 3, pp. 457–474, 2008.

[11] J. Rudolph, *Flatness Based Control of Distributed Parameter Systems*. Aachen, Germany: Shaker Verlag, 2003.

[12] F. Woittennek, *Beiträge zum Steuerungsentwurf für Lineare, Örtlich Verteilte Systeme mit Konzentrierten Stelleingriffen*. Aachen, Germany: Shaker Verlag, 2007.

[13] C. Schmuck, F. Woittennek, A. Gensior, and J. Rudolph, "Flatness-based feed-forward control of an HVDC power transmission network," in *Proc. 33rd Inter Telecommun. Energy Conf.*, Oct. 2011, pp. 1–6.

[14] K. Küpfmüller, W. Mathis, and A. Reibiger, *Theoretische Elektrotechnik*. Berlin, Germany: Springer-Verlag, 2006.

[15] M. Fliess, P. Martin, N. Petit, and P. Rouchon, "Active signal restoration for the telegraph equation," in *Proc. Conf. Decision Control*, 1999, pp. 1107–1111.

Christian Schmuck received the Dipl.-Ing. degree in mechatronics from Technische Universität Dresden, Dresden, Germany, in 2009. He is currently pursuing the Dr.-Ing. degree focussing on the analysis and the control of simulated moving bed processes.

He is currently with the Max Planck Institute for Dynamics of Complex Technical Systems, Magdeburg, Germany, and with the Fachgebiet Regelungssysteme at Technische Universität Berlin, Berlin, Germany. His current research interests include controller and observer design for nonlinear and distributed parameter systems.

Frank Woittennek received the Dipl.-Ing. and Dr.-Ing. degrees in electrical engineering from Technische Universität Dresden (TU Dresden), Dresden, Germany, in 1999 and 2007, respectively.

He was a Post-Doctoral Researcher with the Laboratoire d'Informatique at École Polytechnique, Palaiseau, France, from 2007 to 2008. He is currently responsible for the Distributed Parameter Systems Group, Institute of Control Theory, TU Dresden. His current research interests include analysis, control and observer design for distributed parameter systems, identification of distributed parameter systems, and the control of nonlinear mechanical systems.

Albrecht Gensior received the Dipl.-Ing. and Dr.-Ing. degrees in electrical engineering from Technische Universität Dresden (TU Dresden), Dresden, Germany, in 2003 and 2008, respectively.

He is currently with Professur Leistungselektronik, Elektrotechnisches Institut, TU Dresden, where he is involved in research projects dealing with the control of power electronic converters and drives. His current research interests include nonlinear controller design and observers for these applications.

Joachim Rudolph (M'09) received the Doctorat degree from the Université Paris XI, Orsay, France, in 1991, and the Dr.-Ing. Habil. degree from Technische Universität Dresden (TU Dresden), Dresden, Germany, in 2003.

He has been a Privatdozent with TU Dresden, and was appointed a apl. Professor in 2008. Since 2009, he has been the Head of the Chair of systems theory and control engineering with Saarland University, Saarbrücken, Germany. His current research interests include controller and observer design for nonlinear and infinite dimensional systems, algebraic systems theory, and the solution of demanding practical control problems.